IEEE Access
Multidisciplinary | Rapid Review | Open Access Journal

Received January 9, 2017, accepted January 18, 2017, date of publication January 24, 2017, date of current version March 13, 2017.

Digital Object Identifier 10.1109/ACCESS.2017.2657638

Formulation and Analysis of Grid and Coordinate Models for Planning Wind Farm Layouts

HUAN LONG[1], (Student Member, IEEE), ZIJUN ZHANG[1], (Member, IEEE), ZHE SONG[2], AND ANDREW KUSIAK[3], (Member, IEEE)

[1]Department of Systems Engineering and Engineering Management, City University of Hong Kong, Hong Kong
[2]The School of Business, Nanjing University, Nanjing 210093, China
[3]Department of Mechanical and Industrial Engineering, The University of Iowa, Iowa City, IA, 52242 USA

Corresponding author: Z. Zhang (zijzhang@cityu.edu.hk)

This research was supported in part by an Early Career Scheme grant from the Research Grants Council of Hong Kong (Project No. CityU 138313), in part by a grant from the PROCORE-France/Hong Kong Joint Research Scheme sponsored by the Research Grants Council of Hong Kong and the Consulate General of France in Hong Kong (No.: F-CityU 110/14), in part by a CityU Strategic Research Grant (Grant No. 7004551), as well as in part by National Natural Science Foundation of China (Grant No. 71001050).

ABSTRACT In this paper, a comprehensive study of the effectiveness of the classical grid and coordinate models (CMs) in producing the optimal wind farm layout is conducted based on theoretical analyses and computational experiments. The wind farm layout planning with the grid model (GM) and CM is formulated as a combinatorial and a continuous optimization problem separately. Theoretical analyses prove that it is more complicated to solve CM than GM if the solution space of two models is searched exhaustively. In computational studies, the impact of advanced heuristic search methods on generating optimal wind farm layouts with GM and CM is analyzed. First, two models are solved with the multi-swarm optimization (MSO) algorithm, and CM, in general, produces better layouts, because swarm intelligence is inherently continuous and the flexibility of CM. To further evaluate the importance of selecting an appropriate heuristic search algorithm, the random key genetic algorithm (RKGA) is introduced to compare with MSO in solving GM. Results show that GM produces much better wind farm layouts with RKGA, which is inherently combinatorial. Computational results demonstrate that it is important to match the inherent suitability of heuristic search algorithms with the type of the layout planning models in the wind farm layout optimization.

INDEX TERMS Wind farm, layout planning, heuristic search, comparative analysis, power maximization.

I. INTRODUCTION

Wind turbines are usually distributed over a broad geographical area. The upstream turbines of a wind farm produce wakes affecting downstream turbines [1]. Wind farm layout design researches aim at generating optimal locations of wind turbines to minimize the wake effect and maximize the power output over the life-span of the wind farm.

Studies of the wind farm layout planning are categorized into two groups. The first group focuses on optimization of the wind farm layout with GMs. In [2]–[8], the geographical region of a wind farm is modeled as a grid with a number of columns and rows. Centers of the grid cells are typically considered as potential spots for placing wind turbines. The solution of a GM is a combination of cells with the assigned wind turbines. Mosetti *et al.* [2] studied optimizing wind turbine locations at a site modeled as a 10×10 grid. The authors [2] considered two objectives, the maximization of energy output and minimization of the installation cost. Grady *et al.* [3] investigated the optimization of the wind turbine placement with GMs for different wind directions. Castro Mora *et al.* [4] presented an algorithm for designing a wind farm, including the layout of wind turbines. The major drawback of the grid layout approach is in the optimality of obtained solutions. First, the GM usually locates each wind turbine at the center of a cell which restricts the layout flexibility. Next, the effectiveness of heuristic search algorithms impacts the quality of solutions. To improve the flexibility of the grid layout model, Du Pont and Cagan [5] introduced an extended pattern search approach for solving GMs, thus allowing for more flexible placement of wind turbines. Emami and Noghreh [6] extended the genetic algorithm by incorporating a new coding approach to solve the GM. Long and Zhang [7] presented a two-echelon wind farm layout model to improve the flexibility of GM in the wind farm layout planning. Chen *et al.* [8] developed an innovative optimization method based on the multi-objective genetic algorithm to solve the wind farm layout model.

The second group of topics focused on optimizing the wind farm layout with CMs. These models allow the full freedom of locating wind turbines. In CMs, a wind farm is represented in Cartesian coordinates, and therefore any x-y location can be used for placing wind turbines. Since values

of x and y are continuous, solving the CM is a continuous optimization problem. Kusiak and Song [9] formulated the wind farm layout model based on the coordinate system and proposed an evolutionary strategy algorithm for solving the model. Saavedra-Moreno *et al.* [10] introduced a seeding evolutionary algorithm to solve a CM converted from a GM. Eroglu and Seckiner [11] examined the ant colony algorithm in solving the CM. Perez *et al.* [12] utilized the coordinate system to model the site of an offshore wind farm and introduced a mathematical programming approach to solve it. Chowdhury *et al.* [13] discussed a CM with multiple types of wind turbines. According to [9]–[14], the major researches on CMs have focused on examining the development of solution algorithms.

The wind farm layout optimization has been independently studied based on GMs and CMs [1]–[12]. A comprehensive comparison of the advantages and drawbacks of GM and CM in planning the wind farm layout is seldom [15]. This research offers a thorough investigation of the effectiveness of GM and CM in planning the wind farm layout based on theoretical analyses and computational experiments. The general GM and CM are firstly formulated. The wake effect as well as the uncertainty of the wind speed and direction are considered. The key model difference is that planning the optimal wind farm layout with GM and with CM belong to a combinatorial and a continuous optimization problem separately. The theoretical analyses prove that solving CM with exhaustively searching its solution space is more complicated than solving GM with the same approach. In computational experiments, the impact of advanced heuristic search algorithms on producing wind farm layouts with GM and CM is analyzed. The MSO algorithm is firstly applied to solve both GM and CM. Computational results show that CM solved by MSO generates better layouts than GM. As the swarm intelligence is inherently continuous, solving GM with a solution algorithm which is inherently combinatorial might return better results. The RKGA algorithm is next applied to solve the GM and compared with the MSO. Computational results validate that it is important to choose the suitable solution algorithm based on characteristics of the optimization model in the wind farm layout design.

II. PROBLEM DESCRIPTION

In this section, the wind farm layout planning problem including its assumptions, the considered wake loss model and the wind power generation model is described.

A. BACKGROUND AND ASSUMPTIONS

The following assumptions, A1 – A5, are considered for simple and general layout design cases:

A1. The power curves of wind turbines are identical and their power output characteristics are modeled by a 2-parameter logistic function in (1).

$$P_i = p(v_i) = \begin{cases} 0 & v_i > v_{co}, v_i < v_{ci} \\ \dfrac{e^{v_i}}{a + be^{v_i}} & v_{ci} \le v_i < v_r \\ P_{\max} & v_r \le v_i < v_{co} \end{cases} \quad (1)$$

where P is the power output, $P_{\max}$ is the rated power, v is the wind speed, i is the wind turbine index, v_{co} is the cut-out wind speed, v_{ci} is the cut-in wind speed, v_r is the rated wind speed, and a, b are the parameters of the logistic function (1).

A2. The geographical region for locating wind turbines is a plane.

A3. The minimal distance between two adjacent wind turbines is set to four times of the rotor radius, $4R$.

A4. The wind speed v conditioned on direction θ in the wind farm follows a Weibull distribution described in (2) with the scale parameter λ and the shape parameter k.

$$f_W(v, \lambda, k) = \frac{k}{\lambda}\left(\frac{v}{\lambda}\right)^{k-1} \exp\left(-\left(\frac{v}{\lambda}\right)^{k}\right), \quad \lambda = \lambda'(\theta), k = k'(\theta) \quad (2)$$

A5. The wake produced by a wind turbine expands linearly and forms a conic shape.

B. WAKE EFFECT MODEL

Wind turbines generate wake behind their swept areas as shown in Fig. 1. The wake weakens the kinetic energy of the wind at downstream wind turbines which negatively impact the wind farm power output. Although the elimination of the wake effect is challenging, given the prevailing wind direction, it is possible to minimize the wake effect by the optimal wind farm layout.

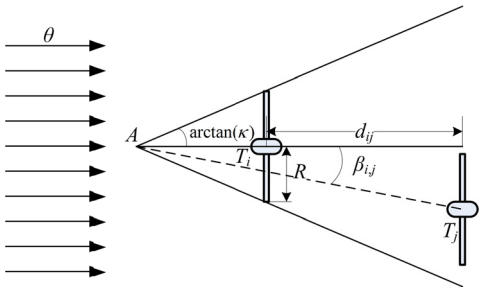

FIGURE 1. Jensen's wake effect model.

To quantify the wake effect in the layout design, the Jensen's wake model introduced in [16] is applied. The wake generated by wind turbine i located at point T_i is modeled as a conic section. The angle $\angle T_iAT_j$ in Fig. 1 identifies turbine j affected by the wake of turbine i, i and $j = 1, 2, \ldots, n$, $i \neq j$. Given the wind direction, θ, the wake expansion constant, κ, coordinates of turbine i, (x_i, y_i), and coordinates of turbine j, (x_j, y_j), the angle, denoted as $\beta_{i,j}$, can be obtained from (3).

$$\beta_{i,j} = \cos^{-1} \times \left[\frac{(x_j - x_i)\cos\theta + (y_j - y_i)\sin\theta + R/\kappa}{\sqrt{(x_j - x_i + \frac{R}{\kappa}\cos\theta)^2 + (y_j - y_i + \frac{R}{\kappa}\sin\theta)^2}}\right] \quad (3)$$

The distribution of the wind speed at wind turbines affected by the wake is re-estimated by Kusiak and Song [9]. It is

demonstrated that only the scale parameter, $\lambda'(\theta)$, of the Weibull distribution is impacted. The new $\lambda'(\theta)$ and new wind speed of affected wind turbine j is estimated by (4) and (5).

$$\lambda'_j(\theta) = \lambda(\theta)(1 - v_j^{def}), \quad j = 1, 2, \ldots, n \tag{4}$$

$$v_j^{def} = \sqrt{\sum_{i=1, i\neq j, \beta_{i,j}<\arctan(\kappa)}^{n} \left[\frac{1-\sqrt{1-C_T}}{(1+\frac{\kappa}{R}d_{i,j})^2}\right]^2} \tag{5}$$

where C_T is the thrust coefficient constant and $d_{i,j}$ describes the distance between turbine i and j projected on θ (see Eq. (6)).

$$d_{i,j} = \left|(x_i - x_j)\cos\theta + (y_i - y_j)\sin\theta\right|. \tag{6}$$

C. WIND POWER GENERATION MODEL

Having computed $\lambda'_j(\theta)$, the expected power output of turbine j can be obtained by integrating the product of (1) and (2) over v and θ as shown in (7). The power output over $[0, v_{ci})$ and $[v_{co}, \infty)$ is 0 because $p(v_j) = 0$ when $v_j \in [0, v_{ci})$ and $[v_{co}, \infty)$.

$$E(P_j) = \int_0^{360^\circ}\int_{v_{ci}}^{v_r} f_\theta(\theta) f_W(v_j, \lambda'_j(\theta), k'(\theta)) \frac{e^{v_i}}{a + be^{v_i}} dv_j d\theta + \int_0^{360^\circ}\int_{v_r}^{v_{co}} f_\theta(\theta) f_W(v_j, \lambda'_j(\theta), k'(\theta)) P_{\max} dv_j d\theta \tag{7}$$

The integration in (7) is challenging as the model has a complex form and the probability distribution function of θ, $f_\theta(\theta)$, is unknown. Numerical integration is applied to obtain an approximate value. Let $\theta_1, \theta_2, \ldots, \theta_h$ be the dividing points of the wind direction with the following order, $\theta_1 \leq \theta_2 \leq \ldots \leq \theta_{h-1} \leq 360$, where $\theta_0 = 0^\circ$ and $\theta_h = 360^\circ$. The wind speed interval, $[v_{ci}, v_r]$, is divided by points, $v_1, v_2, \ldots, v_s$ with the order $v_1 \leq v_2 \leq \ldots \leq v_{s-1} \leq v_r$, where $v_0 = v_{ci}$ and $v_s = v_r$. The expected power output of wind turbine j is approximated as shown in (8).

$$E(P_j) = \sum_{\xi=1}^{h} w_\xi \left\{ \sum_{\psi=1}^{s} \frac{e^{(v_{\psi-1}+v_\psi)/2}}{a + be^{(v_{\psi-1}+v_\psi)/2}} \times \left(e^{-\left(v_{\psi-1}/\lambda'_j((\theta_{\xi-1}+\theta_\xi)/2)\right)^{k'((\theta_{\xi-1}+\theta_\xi)/2)}} - e^{-\left(v_\psi/\lambda'_j((\theta_{\xi-1}+\theta_\xi)/2)\right)^{k'((\theta_{\xi-1}+\theta_\xi)/2)}} \right) + P_{\max}\left(e^{-\left(v_r/\lambda'_j((\theta_{\xi-1}+\theta_\xi)/2)\right)^{k'((\theta_{\xi-1}+\theta_\xi)/2)}} - e^{-\left(v_{co}/\lambda'_j((\theta_{\xi-1}+\theta_\xi)/2)\right)^{k'((\theta_{\xi-1}+\theta_\xi)/2)}} \right) \right\} \tag{8}$$

III. WIND FARM LAYOUT MODELS

In this section, general grid and coordinate wind farm layout models are separately formulated.

A. GRID MODEL

The geographical region of a wind farm is modeled as a grid composed of equal size cells. The center of each cell is considered as the potential spot for locating a wind turbine. Let a variable, $l_{n'm'} \in \{0, 1\}$, $n' = 1, 2, \ldots, N$, $m' = 1, 2, \ldots, M$, denote the decision of selecting cells in row n' and column m' for locating wind turbines, the GM becomes a combinatorial optimization model formulated in (9).

The equality constraint in (9) states that the total number of selected cells should be equal to the total number of wind turbines. The inequality constraint says that the total number of cells in the grid needs to be larger than the total number of wind turbines. To compute $E(P_{n'm'})$ by (8), centers of the selected cells are transformed in a set of two dimensional coordinates, $(x_{n'm'}, y_{n'm'})$.

$$\begin{aligned} \max \ & \sum_{n'=1}^{N}\sum_{m'=1}^{M} l_{n'm'} E(P_{n'm'}) \\ \text{s.t.} \ & \sum_{n'=1}^{N}\sum_{m'=1}^{M} l_{n'm'} = n \\ & MN \geq n \\ & l_{n'm'} \in \{0, 1\}, \quad n' = 1, 2, \ldots, N, m' = 1, 2, \ldots, M \end{aligned} \tag{9}$$

B. COORDINATE MODEL

The CM is more flexible than the GM. The region for developing a wind farm is represented by an infinite set of 2-dimensional coordinates. Each coordinate represents for a potential location of a wind turbine. Let (x_i, y_i) denote the position of wind turbine i, $i = 1, 2, \ldots, n$, x_l be the lower bound of x_i, x_u be the upper bound of x_i, y_l be the lower bound of y_i, and y_u be the upper bound of y_i, the wind farm layout planning based on the coordinate system is a continuous optimization model as expressed in (10).

$$\begin{aligned} \max \ & \sum_{i=1}^{n} E(P_i) \\ \text{s.t.} \ & x_l + R \leq x_i \leq x_u - R \\ & y_l + R \leq y_i \leq y_u - R \\ & (x_i - x_j)^2 + (y_i - y_j)^2 \geq 64R^2, \quad \forall i, j, i \neq j \\ & i, j = 1, 2, \ldots, n \end{aligned} \tag{10}$$

In (10), the constraint, $(x_i - x_j)^2 + (y_i - y_j)^2 \geq 64R^2$, is applied to guarantee a safe distance, $4R$, between wind turbines i and j. In GM, such safe distance is automatically satisfied by the appropriate design of cell size.

IV. MODEL ANALYSIS

The advantages and drawbacks of GM and CM in planning the wind farm layout are theoretically studied in this section. It is intuitively obvious that GM offers a subset of solutions of CM and is less flexible in locating wind turbines. Due to the complexity of both GM and CM, they have been widely solved with heuristic search algorithms.

Thus, it is interesting to study the complexity of solving two models heuristically. To facilitate the theoretical analysis, the simplest heuristic procedure that all feasible solutions of two models are exhaustively searched without replication to obtain the optimal solution is considered. We can prove that theoretically it is more complicated to solve CM than GM with the exhaustive search through **Lemma 1 – 4**:

Lemma 1: The number of feasible solutions for distributing n wind turbines into an $M \times N$ grid is C^n_{MN}, where $n \leq MN$.

Proof: The combination of distributing n wind turbines into an $M \times N$ grid is equivalent to the combination of selecting n out of total MN cells. It is intuitively obvious that the number of feasible solutions is the number of combinations without repetitions and orders, which is $\frac{MN!}{n!(MN-n)!} = C^n_{MN}$.

Lemma 2: Given a rectangular wind farm site approximated as an $M' \times N'$ matrix containing $M'N'$ pairs of x-y coordinates, where M' and N' are large numbers, and a set of minimal distance constraints, $(x_i - x_j)^2 + (y_i - y_j)^2 \geq 64R^2$, $\forall i, j, i \neq j$, the number of feasible solutions of CM needs to be searched is $\prod_{i=1}^{n} C^1_{M'N'-\sum_{j=0}^{i-1} K_j-(i-1)}$ by assuming that minimal distance constraints indicate mutually exclusive regions of K_i pairs of coordinates, $i = 1, 2, \ldots, n$, infeasible for locating any other wind turbines after installing the i^{th} wind turbine.

Proof: Given a site for planning the wind farm layout approximating by a set of $M'N'$ pairs of x-y coordinates, $\{(x_1, y_1), (x_1, y_2), \ldots, (x_{M'}, y_{N'})\}$, the assignment of wind turbines into this site is equivalent to the selection of n out of $M'N'$ pairs of x-y coordinates without repetitions. However, due to the constraint, $(x_i - x_j)^2 + (y_i - y_j)^2 \geq 64R^2$, $\forall i, j$, $i \neq j$, K_i pairs of x-y coordinates forming a round region will be infeasible for assigning next wind turbine after the region center, (x_i, y_i), is selected to locate the wind turbine i, shown as Fig. 2(a).

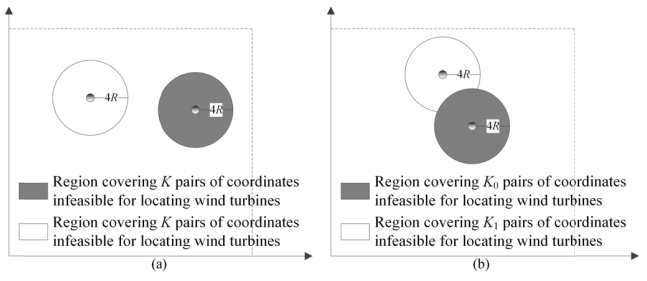

FIGURE 2. Two scenarios of infeasible regions for locating wind turbines.

The selection order matters because K_i pairs of coordinates, $i = 1, 2, .., n$, might not form a full circle. It is because that the infeasible round regions could overlap as shown in Fig. 2(b) and the order impacts the size of K_i. For $i = 1$, the number of feasible solutions is $C^1_{M'N'}$. For $i = 2$, the number of feasible solutions is $C^1_{M'N'}C^1_{M'N'-K_1-1}$. For $i = 3$, the number of feasible solutions is $C^1_{M'N'}C^1_{M'N'-K_1-1}C^1_{M'N'-K_1-K_2-2}$. Following this pattern, it can be inferred that when $i = n$, the number of feasible solutions is $C^1_{M'N'}C^1_{M'N'-K_1-1}C^1_{M'N'-K_1-K_2-2}\cdots C^1_{M'N'-K_1-K_2\cdots-K_{n-1}-(n-1)} = \prod_{i=1}^{n} C^1_{M'N'-\sum_{j=0}^{i-1} K_j-(i-1)}$.

Lemma 3: The least number of feasible solutions of the coordinate model needs to be searched given a site approximated as $M'N'$ pairs of x-y coordinates is $\prod_{i=1}^{n} C^1_{M'N'-(i-1)K-(i-1)}$, where $K = \max\{K_0, K_1, \ldots, K_{n-1}\}$ and the constraint, $(x_i - x_j)^2 + (y_i - y_j)^2 \geq 64R^2$, indicates a round region covering K pairs of x-y coordinates infeasible for installing wind turbines, $\forall i, j, i \neq j$.

Proof: Assume a best case (e.g. Fig. 2(a)) that each constraint, $(x_i - x_j)^2 + (y_i - y_j)^2 \geq 64R^2$, covers an identical and independent round region containing K pairs of x-y coordinates infeasible for installing any other wind turbines after the i^{th} turbine is placed, $\forall i, j, i \neq j, K \geq \max\{K_0, K_1, \ldots, K_{n-1}\}$, the number of feasible solution is $\prod_{i=1}^{n} C^1_{M'N'-(i-1)K-(i-1)}$. Since $K \geq \max\{K_0, K_1, \ldots, K_{n-1}\}$, $C^1_{M'N'-(i-1)K-(i-1)} \leq C^1_{M'N'-\sum_{j=0}^{i-1} K_j-(i-1)}$, $\forall i$. Next, we can obtain that $\prod_{i=1}^{n} C^1_{M'N'-(i-1)K-(i-1)} / \prod_{i=1}^{n} C^1_{M'N'-\sum_{j=0}^{i-1} K_j-(i-1)} \leq 1$ which proves that $\prod_{i=1}^{n} C^1_{M'N'-(i-1)K-(i-1)}$ is the least number of feasible solutions offered by the coordinate model.

Lemma 4: If $M'N' - (n-1)K \geq MN$, the total number of feasible solutions of the coordinate model needs to be searched in the benchmark heuristic procedure is larger than that of the grid model.

Proof: The number of feasible solutions of grid and coordinate models is compared by evaluating (11).

$$\begin{aligned}
&\frac{C^n_{MN}}{\prod_{i=1}^{n} C^1_{M'N'-(i-1)K-(i-1)}} \\
&= \frac{[MN(MN-1)\cdots(MN-(n-1))]/n!}{M'N'(M'N'-K-1)\cdots(M'N'-(n-1)K-(n-1))} \\
&\leq \frac{[MN(MN-1)\cdots(MN-(n-1))]}{M'N'(M'N'-K-1)\cdots(M'N'-(n-1)K-(n-1))}
\end{aligned} \tag{11}$$

The $\frac{MN}{M'N'} \leq \frac{MN-1}{M'N'-K-1} \leq \cdots \leq \frac{MN-(n-1)}{M'N'-(n-1)K-(n-1)}$ holds for $K > 1$. The value $K > 1$ is obvious because of the constraint, $(x_i - x_j)^2 + (y_i - y_j)^2 \geq 64R^2$, $\forall i, j$, $i \neq j$. In this case, $\frac{MN-(n-1)}{M'N'-(n-1)K-(n-1)} < 1$ can infer that $\frac{[MN(MN-1)\cdots(MN-(n-1))]}{M'N'(M'N'-K-1)\cdots(M'N'-(n-1)K-(n-1))} < 1$, which means $\frac{C^n_{MN}}{\prod_{i=1}^{n} C^1_{M'N'-(i-1)K-(i-1)}} < 1$. Therefore, one can conclude that if the condition, $M'N' - (n-1)K > MN$, is met, the total number of feasible solutions of the CM needs to be searched is larger than that of the GM.

V. MULTI-SWARM OPTIMIZATION ALGORITHM

Exhaustive search is simple but inefficient. In previous studies, advanced heuristic search algorithms, such as variants of the genetic algorithm and swarm intelligence, were widely employed to solve wind farm layout models [1]–[12]. It is challenging to theoretically analyze their impacts on solving GM (9) and CM (10) due to the algorithm complexity. Thus, such analysis is explored through extensive computational experiments. Based on (9) and (10), it is explicit that solving GM and CM belong to a constrained combinatorial and a continuous optimization problem separately since decision variables in (9) and (10) are binary and continuous. To conduct a fair computational experiment, a powerful swarm intelligence, the multi-swarm optimization (MSO) algorithm [17], is adapted to solve GM and CM.

The MSO algorithm is revised from the classical particle swarm optimization (PSO) algorithm [18], while the particle evolution principle remains the same as descripted by (12).

$$\begin{aligned} \mathbf{U}_i &= \varpi \mathbf{U}_{i-1} + c_1 r_1(\mathbf{lbest}_{i-1} - \mathbf{x}_{i-1}) - c_2 r_2(\mathbf{gbest} - \mathbf{x}_{i-1}) \\ \mathbf{x}_i &= \mathbf{x}_{i-1} + \mathbf{U}_i \end{aligned} \tag{12}$$

where $\mathbf{U}$ is a vector of the velocity of a particle, $\mathbf{x}$ is a vector describes the position of a particle, **lbest** describes the local best solution, **gbest** is the global best solution, i is the index of search generations, ϖ is the inertia weight, c_1, c_2 are two acceleration constants, as well as r_1, r_2 are randomly generated from $U(0, 1)$. To update the **lbest** and **gbest**, the fitness of local and global bests is compared with the fitness of particles' positions. If the fitness of a particle's position is better, the local and global bests will be replaced by the particle's position.

Compared with the PSO, which groups all particles into a single swarm, particles in MSO form multiple small swarms. These swarms are continuously regrouped over search iterations to exchange information among swarms. All particles are grouped into a single swarm to perform the ordinary PSO search at the end of search iterations. The principle of MSO offers better diversification during the search process and prevents the early convergence.

The procedure of MSO includes the following steps:

Step 1 Initialize positions and velocities of $s_1 \times s_2$ particles given the swarm size, s_1, and the number of swarms, s_2. Randomly assign all particles into s_2 swarms.

Step 2 Repeat Steps 2.1 – 2.3 until the number of generations exceeds 0.9 of the maximal generation, N_{mso}.

Step 2.1 Evaluate the fitness of all particles and update their positions and velocities of s_2 swarms by (12).

Step 2.2 Update **lbest** and **gbest** of s_2 swarms.

Step 2.3 Regroup swarms if the regrouping condition is satisfied.

Step 3 Group all particles into a swarm and repeat Steps 3.1 - 3.2 until N_{mso} is reached.

Step 3.1 Evaluate the fitness of all particles and update their positions and velocities by (12).

Step 3.2 Update **lbest** and **gbest**.

Since the MSO is inherently continuous, it cannot directly solve the GM (9). Thus, the MSO is extended by integrating the binary PSO introduced by Kennedy and Eberhart [19] to offer the operation in the binary space and to solve the GM (9). It uses the concept of velocity as a probability that a position takes on 1 or 0. Updating the velocity in (12) remained unchanged. The update of the position is implemented by (13).

$$\begin{aligned} \upsilon_i &= \varpi \upsilon_{i-1} + c_1 r_1(lbest_{i-1} - x_{i-1}) - c_2 r_2(gbest - x_{i-1}) \\ x_i &= \begin{cases} 0 & if\ \text{rand}() \geq S(\upsilon_i) \\ 1 & if\ \text{rand}() < S(\upsilon_i) \end{cases} \end{aligned} \tag{13}$$

where $S(\cdot)$ is the sigmoid function for transforming the velocity into the probability and rand() is an operator randomly generating numbers from a uniform distribution over [0, 1]. In the discrete version, it appears that υ_i functions as a probability threshold.

VI. COMPUTATIONAL STUDIES

The capability of GM and CM in producing optimal wind farm layouts is examined through computational experiments considering two wind scenarios. Moreover, a variety of cases are developed based on various wind turbine numbers, 10 – 25, as well as the side length of grid cells ranging from $4.5R$ to $12.5R$. The combinatorial and continuous versions of MSO are firstly applied to address GM and CM respectively. As MSO is inherently continuous, the random keys genetic algorithm (RKGA) [20], which is inherently combinatorial, is next compared with the MSO in solving GM, which is a combinatorial optimization problem. Heuristic search algorithms can converge to different local optima over multiple runs due to the stochasticity in the iterative search. To provide an overall computational performance, the experiment is repeatedly implemented five times for each case. The computational results including the maximal power output, the average power output, and the average running time of five repetitions of solving GM and CM are reported and analyzed.

A. PARAMETER SETTINGS

The parameters of the wind farm layout and the algorithms used in this research are fixed as follows for all computational experiments. The site is a square with a 2000×2000 m^2 area. The GE1.5-77 turbine with a rated power of 1500 kW is considered in the layout design. The parameters of the wind turbine and MSO algorithm are respectively specified in Tables 1 and 2.

B. COMPUTATIONAL STUDY 1

The wind scenario 1 (WS1) is considered in this section. In WS1, the wind distribution is relatively simple and the prevailing wind direction is obvious. The characteristics of WS1 are described in Table 3. According to Table 3, the wind blows predominantly in directions from 75° to 105° with a probability of 0.8. In experiments of WS1, the number of grid cells varies from 5×5 to 11×11.

TABLE 1. Parameter settings of wind turbines.

Param	*Explanation*	*Value*
z	Hub height of WT (m)	80
R	Rotor radius of WT (m)	40
C_T	Thrust coefficient of WT (m)	0.8
κ	Environment constant	0.1
v_{ci}	Cut-in speed of WT (m/s)	3.5
v_r	Rated speed of WT (m/s)	14
v_{co}	Cut-out speed of WT (m/s)	25
a	Parameter of power curve function	6.0268
b	Parameter of power curve function	0.0007

TABLE 2. Parameter settings of MSO algorithm.

Param	*Explanation*	*Value*
s_1	Size of a swarm	10
s_2	Number of swarm	5
ϖ	Inertia weight	0.9
c_1	Acceleration constant	2
c_2	Acceleration constant	2
N_{mso}	Number of iterations	5000

TABLE 3. Wind scenario 1.

i	θ_i	θ_{i+1}	k	c	w_ξ	i	θ_i	θ_{i+1}	k	c	w_ξ
0	0	15	2	13	0	12	180	195	2	13	0.01
1	15	30	2	13	0.01	13	195	210	2	13	0.01
2	30	45	2	13	0.01	14	210	225	2	13	0.01
3	45	60	2	13	0.01	15	225	240	2	13	0.01
4	60	75	2	13	0.01	16	240	255	2	13	0.01
5	**75**	**90**	**2**	**13**	**0.2**	17	255	270	2	13	0.01
6	**90**	**105**	**2**	**13**	**0.6**	18	270	285	2	13	0.01
7	105	120	2	13	0.01	19	285	300	2	13	0.01
8	120	135	2	13	0.01	20	300	315	2	13	0.01
9	135	150	2	13	0.01	21	315	330	2	13	0.01
10	150	165	2	13	0.01	22	330	345	2	13	0.01
11	165	180	2	13	0.01	23	345	360	2	13	0

TABLE 4. Maximal power output of GM and CM in WS1 under MSO.

n	GM							CM
	5×5	6×6	7×7	8×8	9×9	10×10	11×11	
10	8700.22	8727.42	8727.63	8727.78	8713.99	**8730.45**	8723.51	8776.87
11	9521.75	9555.63	9577.01	9559.34	9572.54	**9590.93**	9571.40	9637.20
12	10337.61	10397.44	**10424.32**	10413.61	10413.29	10424.24	10421.06	10492.98
13	11153.86	11211.21	11242.41	11236.23	11252.88	**11278.63**	11261.22	11339.98
14	11967.73	12028.94	**12110.45**	12069.73	12084.38	12107.94	12107.06	12208.81
15	12779.91	12871.37	12880.30	12892.85	12923.26	**12954.55**	12927.65	13044.28
16	**13942.96**	13659.67	13718.01	13702.94	13712.44	13746.60	13756.78	13864.40
17	14206.20	14467.49	14499.16	14476.23	14548.12	**14594.69**	14552.99	14676.04
18		15237.86	15309.07	15293.33	15320.82	**15375.31**	15370.62	15538.33
19		16026.24	16107.46	16082.79	16129.60	16173.50	**16174.31**	16333.31
20		16750.55	16878.83	16821.58	16930.16	16956.53	**17019.27**	17144.45
21		17473.76	17628.92	17624.12	17689.99	17742.23	**17783.35**	17980.63
22		18194.29	18371.40	18355.12	18494.96	18487.13	**18531.56**	18765.76
23		18913.38	19106.78	19116.07	19205.87	19297.03	**19337.17**	19549.28
24		19625.99	19828.35	19852.27	19969.08	20048.98	**20070.78**	20402.49
25		20289.62	20583.09	20572.31	20742.62	**20908.20**	20836.64	21132.38

The computational results of solving GM and CM with different wind turbine numbers and grid designs are presented in Tables 4 – 6. In Table 4, it is observable that the maximal and average power output of CM is better than the best one of GM for all cases. The advantage of CM is more obvious with increasing the number of the wind turbines, e.g., $n = 19 - 25$. It is because that CM allows more flexible layout design and the MSO algorithm is inherently continuous.

In Table 6, since GM and CM are solved by the same algorithm, MSO, their computational time is close. Solving GM is slightly more computationally intensive than solving CM with MSO because the update of the particle's position in the discrete MSO requires extra operations.

TABLE 5. Average power output of GM and CM in WS1 under MSO.

n	GM							CM
	5×5	6×6	7×7	8×8	9×9	10×10	11×11	
10	8697.56	8714.93	8726.38	8716.70	8713.81	**8730.45**	8718.07	8769.11
11	9520.76	9547.23	9571.30	9559.01	9568.10	9586.24	9569.75	9622.98
12	10337.54	10386.14	**10421.73**	10404.31	10406.53	10418.60	10413.83	10480.20
13	11153.39	11211.21	11242.27	11228.21	11248.30	**11278.63**	11256.02	11326.11
14	11967.73	12021.53	12082.17	12069.73	12072.22	**12101.28**	12090.54	12172.07
15	12779.91	12871.37	12872.78	12886.38	12907.28	**12928.18**	12925.04	13008.44
16	13582.98	13648.78	13697.48	13695.88	13712.44	**13746.60**	13734.66	13838.19
17	14206.20	14451.38	14471.66	14466.40	14524.79	**14563.88**	14544.91	14659.24
18		15205.6	15283.68	15258.16	15320.82	15357.36	**15360.27**	15483.97
19		16004.10	16107.46	16059.22	16109.65	**16155.16**	16149.46	16301.67
20		16745.90	16862.76	16811.96	16899.52	16947.55	**16961.66**	17121.71
21		17471.93	17594.82	17624.12	17647.21	17742.23	**17783.35**	17929.30
22		18192.93	18315.92	18332.35	18431.26	18487.13	**18508.02**	18726.23
23		18911.62	19088.53	19084.97	19174.15	19239.20	**19300.03**	19507.46
24		19622.87	19819.76	19848.28	19911.88	20018.54	**20051.51**	20308.63
25		20289.14	20562.37	20528.73	20659.15	20826.55	**20836.64**	21082.86

TABLE 6. Average running time of GM and CM in WS1 under MSO.

n	GM							CM
	5×5	6×6	7×7	8×8	9×9	10×10	11×11	
10	768.16	763.30	757.95	763.31	763.01	766.28	767.95	713.75
11	834.60	876.56	842.89	841.60	844.69	845.05	845.06	785.86
12	922.77	927.63	917.11	919.39	920.63	921.36	920.13	857.58
13	988.65	989.92	984.93	990.33	999.91	988.56	995.12	944.87
14	1058.02	1060.05	1059.62	1064.06	1067.87	1073.01	1069.75	1010.52
15	1150.36	1152.27	1151.29	1154.19	1155.26	1156.13	1156.83	1088.54
16	1241.12	1239.55	1238.43	1238.87	1242.46	1236.99	1228.76	1168.87
17	1315.10	1316.88	1317.02	1319.16	1322.26	1323.31	1325.25	1251.34
18		1405.11	1405.32	1388.67	1409.36	1410.79	1412.69	1336.90
19		1496.61	1496.26	1498.78	1502.14	1501.45	1502.46	1421.78
20		1588.99	1612.92	1566.33	1602.14	1593.61	1597.70	1513.64
21		1683.06	1682.91	1683.95	1685.17	1687.53	1685.68	1590.41
22		1778.44	1783.18	1782.98	1787.44	1769.75	1770.44	1696.12
23		1871.53	1857.02	1866.47	1872.83	1880.78	1846.48	1783.51
24		1941.79	1968.12	1972.65	1953.22	1952.84	1953.25	1887.71
25		2048.31	2049.11	2048.76	2047.65	2055.48	2056.45	1973.55

Moreover, as shown in Tables 3 and 4, when wind turbine number is low, the power output slightly decreases with the increase of grid cells, e.g., $n = 10$, 11 and 12. It is because that the heuristic algorithm is trapped by the local optimum. Thus, it is valuable to choose the appropriate grid number to provide the best performance of solving GM with MSO.

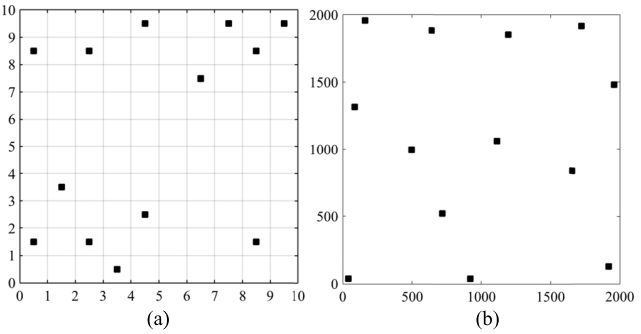

FIGURE 3. Best layout of GM and CM with $n = 13$ in WS1 under MSO. (a) GM. (b) CM.

When the number of wind turbines is low, such as, $n = 13$ in Fig. 3, locations of wind turbines produced by both of GM and CM can indicate the predominant wind direction.

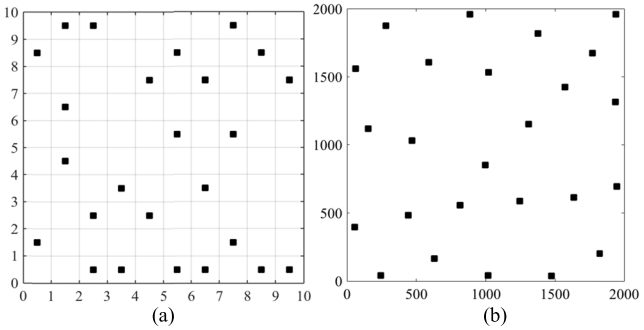

FIGURE 4. Best layout of GM and CM with $n = 25$ in WS1 under MSO. (a) GM. (b) CM.

When the number of wind turbines is larger, such as $n = 25$ in Fig. 4, the predominant wind direction becomes less obvious. Compared with the layout offered by GM, wind turbines in layout of CM stayed far away from their neighbors. Such observation indicates that CM solved MSO can offer more meaningful layout.

C. COMPUTATIONAL STUDY 2

This section discusses computational experiments based on the wind scenario 2 (WS2). In WS2, the predominant wind direction covers a wider range than that of WS1, such as, from 120° to 225°. The details of WS2 are presented in Table 7.

TABLE 7. Wind scenario 2.

i	θ_i	θ_{i+1}	k	c	w_ξ	i	θ_i	θ_{i+1}	k	c	w_ξ
0	0	15	2	7	0.0003	**12**	**180**	**195**	**2**	**10**	**0.1909**
1	15	30	2	5	0.0072	**13**	**195**	**210**	**2**	**8.5**	**0.1162**
2	30	45	2	5	0.0237	**14**	**210**	**225**	**2**	**8.5**	**0.0793**
3	45	60	2	5	0.0242	15	225	240	2	6.5	0.0082
4	60	75	2	5	0.0222	16	240	255	2	4.6	0.0041
5	75	90	2	4	0.0301	17	255	270	2	2.6	0.0008
6	90	105	2	5	0.0397	18	270	285	2	8	0.0010
7	105	120	2	6	0.0268	19	285	300	2	5	0.0005
8	**120**	**135**	**2**	**7**	**0.0626**	20	300	315	2	6.4	0.0013
9	**135**	**150**	**2**	**7**	**0.0801**	21	315	330	2	5.2	0.0031
10	**150**	**165**	**2**	**8**	**0.1025**	22	330	345	2	4.5	0.0085
11	**165**	**180**	**2**	**9.5**	**0.1445**	23	345	360	2	3.9	0.0222

TABLE 8. Maximal power output of GM and CM in WS2 under MSO.

n	GM							CM
	5×5	6×6	7×7	8×8	9×9	10×10	11×11	
10	4125.04	4131.09	**4140.61**	4124.31	4127.24	4139.08	4131.23	4185.38
11	4516.03	4502.84	**4548.07**	4507.74	4512.48	4522.55	4532.67	4587.36
12	4882.86	4908.43	4906.87	4896.09	4883.90	**4918.40**	4904.96	4965.44
13	5242.24	5265.15	**5284.65**	5269.14	5269.17	5266.40	5280.22	5349.02
14	5600.81	5624.46	5640.57	5623.28	5628.77	**5677.36**	5645.32	5711.40
15	5952.71	5988.75	**6048.32**	6012.18	6006.81	6017.69	5993.69	6077.03
16	6263.19	6346.27	**6405.68**	6342.23	6347.25	6362.73	6382.17	6453.62
17	6572.55	6671.47	**6751.45**	6697.27	6694.60	6735.70	6688.78	6796.83
18		**7058.52**	7040.24	7029.76	7053.90	7037.58	7050.45	7143.01
19		7369.13	**7430.89**	7359.97	7379.59	7430.6	7358.00	7498.56
20		7691.77	7720.23	7676.39	7725.19	**7731.76**	7689.95	7793.25
21		7992.83	8067.46	7990.85	8053.11	**8090.64**	7986.92	8137.87
22		8288.07	**8360.49**	8296.32	8330.31	8356.72	8355.17	8458.09
23		8673.24	**8747.53**	8661.60	8633.89	8702.82	8640.11	8803.65
24		8867.81	9033.72	8939.50	8955.89	8990.85	**9258.26**	9083.17
25		9154.46	9321.73	9156.46	9282.10	**9348.31**	9246.32	9445.24

The computational results of various cases in WS2 are reported in Tables 8 – 9. Since the computational time in WS2 is almost the same as the WS1, it is not specified here. Based on results, the performance of CM is still better than GM in most cases, except $n = 24$, and the difference becomes more significant with increasing the number of wind turbines. Yet, the advantage of CM is less obvious in WS2 than WS1.

TABLE 9. Average power output of GM and CM in WS2 under MSO.

n	GM							CM
	5×5	6×6	7×7	8×8	9×9	10×10	11×11	
10	4115.09	4131.09	**4134.94**	4120.36	4116.57	4122.31	4121.40	4178.82
11	4507.11	4498.81	**4524.39**	4493.24	4506.50	4507.79	4517.39	4568.73
12	4880.07	4884.16	**4906.84**	4889.57	4883.90	4889.91	4888.78	4936.10
13	5242.15	5248.75	5270.58	5251.88	5264.49	5259.23	**5280.22**	5324.96
14	5600.81	5612.85	5632.09	5605.16	5618.61	**5677.36**	5631.29	5685.17
15	5952.71	5968.21	5997.38	5983.52	**5998.11**	5992.52	5966.44	6061.51
16	6263.19	6330.28	**6355.26**	6310.35	6325.89	6337.28	6339.58	6439.71
17	6572.55	6660.85	6712.54	6645.61	6694.60	**6715.02**	6676.70	6762.99
18		7033.42	7012.45	6999.39	**7037.27**	7025.61	7031.74	7118.46
19		7356.18	**7390.01**	7310.90	7362.18	7364.92	7339.85	7464.07
20		7684.46	**7698.73**	7657.71	7676.61	7697.41	7679.24	7778.60
21		7985.05	8067.46	7943.54	8022.26	**8080.44**	7964.71	8114.43
22		8283.73	**8355.29**	8296.32	8309.54	8342.18	8314.96	8441.17
23		8568.03	**8698.11**	8558.33	8623.85	8657.61	8614.45	8759.22
24		8859.96	9026.24	8905.27	8955.89	8968.71	**9109.82**	9058.82
25		9153.66	9296.15	9137.67	9220.40	**9297.22**	9240.64	9393.17

In WS2, the 7×7 grid is usually chosen as the best grid for GM. It is because that the predominant wind direction of WS2 covers a wide range. It makes the heuristic algorithm prefer a larger size grid where wind turbines stay far away from each other in all directions.

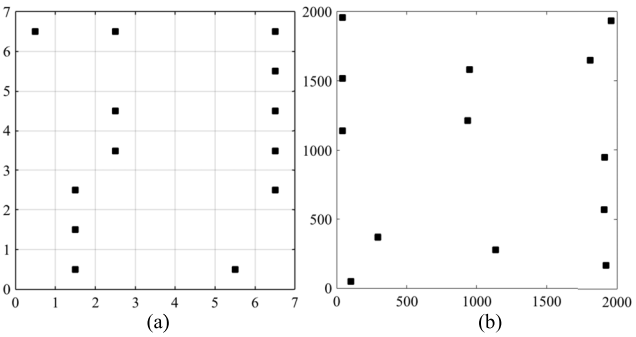

FIGURE 5. Best layout of GM and CM with $n = 13$ in WS2 under MSO. (a) GM. (b) CM.

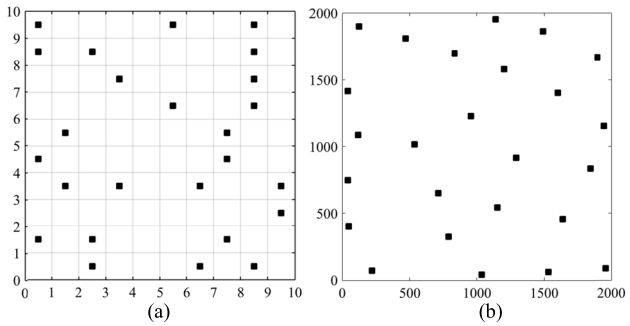

FIGURE 6. Best layout of GM and CM with $n = 25$ in WS2 under MSO. (a) GM. (b) CM.

The best wind farm layouts produced by two models with $n = 13$ and 25 are shown in Figs. 5 and 6. When $n = 13$,

both of the layouts of GM and CM can indicate the predominant wind direction. When $n = 25$, both of GM and CM layouts intend to evenly allocate wind turbines over the space.

Based on the results in WS1 and WS2, the CM obtains the better performance than GM with the MSO algorithm. Besides the flexibility of CM, the MSO, which is inherently continuous, can also impact the quality of solutions obtained by solving the GM, which is a combinatorial optimization problem. Thus, the inherent suitability of heuristic algorithms can influence the solution quality of the same model and it will be explored in the next section.

D. COMPUTATIONAL STUDY 3

In previous studies [2], [3], [6] considering GM in the wind farm layout design, the genetic algorithm (GA) was commonly considered. Here, an improved GA algorithm, the RKGA, is employed to compare with the discrete MSO in solving the GM.

The RKGA introduced random keys to ingeniously maintain solution feasibility over search iterations. In RKGA, random keys, which are usually random number generated from the [0, 1] uniform distribution, replaces binary variables in the generic GA to form the solution. A decoder next converts random keys to binary values. In the decoder, values in the random keys space are mapped with values in the literal space for the fitness evaluation.

TABLE 10. Parameter settings of RKGA algorithm.

Param	*Value*
Size of *parent* set	50
Size of *offspring* set	150
Size of *mutation* set	25
Crossover probability	0.5
Number of iterations	150

TABLE 11. Maximal power output of GM in WS1 under RKGA.

n	GM						
	5×5	6×6	7×7	8×8	9×9	10×10	11×11
10	**8760.98**	8744.35	8739.03	8748.50	8737.09	8733.22	8736.39
11	9597.69	**9607.12**	9575.23	9578.36	9595.53	9595.67	9528.22
12	**10434.40**	10434.02	10413.85	10397.22	10403.55	10407.81	10423.16
13	11271.11	11243.23	11201.13	11223.14	**11284.19**	11267.11	11192.28
14	**12095.86**	12075.72	12027.10	12056.02	12105.98	12060.08	12027.61
15	12920.61	12907.49	12810.66	12874.32	**12927.35**	12869.95	12792.09
16	12807.52	**13722.25**	13630.33	13690.56	13710.00	13665.19	13620.78
17	12694.43	14531.39	14383.98	14450.35	**14680.08**	14470.13	14256.29
18		15317.06	15456.02	15439.09	15521.67	**15542.20**	15539.18
19		16037.00	16279.90	16245.02	16328.13	16373.99	**16385.24**
20		16760.01	17067.77	17037.02	17135.98	**17200.05**	17192.89
21		17477.98	17862.53	17818.16	17989.61	18020.04	**18025.20**
22		18198.61	18650.34	18710.08	18715.23	18792.98	**18894.67**
23		18916.11	19385.95	19373.21	19515.35	19600.09	**19663.10**
24		19631.96	20105.86	20130.91	20280.36	20427.32	**20463.98**
25		20287.12	20860.60	20910.35	21065.45	21187.14	**21239.73**

The stopping criterion in this paper is the number of iterations. The decoder is a direct mapping between the random keys and the binary solution. Since the number of turbines is n, the number of variables $= 1$ in one solution is n and the number of variables $= 0$ is $MN - n$. The decoder converts the n largest random keys to 1 and the left random keys to 0 to automatically guarantee the solution feasibility. Table 10 describes the detailed parameter settings of the RKGA algorithm.

In Tables 11 – 13, computational results of the RKGA in WS1 are presented. According to results of Tables 11 – 12, the RKGA has better performance than MSO in solving GM. In addition, the results are even better than those of the CM. Such observation indicates that selecting the suitable heuristic algorithm can boost the performance of models.

TABLE 12. Average power output of GM in WS1 under RKGA.

n	GM						
	5×5	6×6	7×7	8×8	9×9	10×10	11×11
10	**8760.98**	8740.12	8703.66	8732.46	8728.93	8717.82	8705.36
11	**9597.69**	9589.32	9553.07	9560.00	9584.89	9569.41	9513.21
12	**10434.40**	10420.22	10394.98	10387.23	10400.40	10394.04	10388.41
13	**11271.11**	11243.23	11183.02	11220.00	11234.07	11225.19	11140.12
14	**12095.86**	12073.23	12010.96	12030.81	12082.94	12020.97	11900.23
15	**12920.61**	12903.28	12788.45	12855.14	12895.91	12790.32	12730.96
16	12807.52	**13722.25**	13575.13	13653.71	13661.07	13560.35	13385.27
17	12694.43	14531.28	14299.60	14379.06	**14616.95**	14318.34	14155.88
18		15310.47	15455.92	15433.76	15510.77	**15530.01**	15517.23
19		16033.92	16272.27	16235.17	16311.31	**16355.09**	16350.91
20		16759.06	17055.10	17026.50	17112.75	17179.52	**17185.69**
21		17476.97	17853.01	17794.87	17911.96	17989.07	**18015.03**
22		18193.03	18639.99	18597.38	18688.14	18783.62	**18848.44**
23		18912.09	19378.65	19351.94	19484.19	19587.71	**19641.70**
24		19629.34	20090.15	20121.76	20272.44	20295.33	**20413.99**
25		20286.37	20835.40	20878.32	21035.75	21161.32	**21200.90**

TABLE 13. Average running time of GM in WS1 under RKGA.

n	GM						
	5×5	6×6	7×7	8×8	9×9	10×10	11×11
10	86.98	87.90	89.62	89.16	90.19	91.18	92.77
11	94.92	95.81	97.56	97.26	97.69	99.87	101.14
12	103.45	103.60	105.25	104.94	106.54	107.80	109.33
13	112.27	112.60	114.12	114.22	115.32	115.73	117.14
14	121.03	122.97	122.09	122.83	123.27	124.17	126.44
15	129.30	130.71	131.37	131.75	132.83	134.14	135.03
16	138.11	138.79	140.43	140.43	142.22	143.73	143.49
17	147.57	148.02	149.95	149.52	150.56	151.96	154.09
18		159.28	160.56	159.36	161.12	162.57	163.88
19		168.79	170.54	169.42	170.17	171.43	173.26
20		179.59	180.07	180.39	180.02	181.61	182.85
21		188.87	189.63	189.99	190.52	192.48	194.96
22		199.89	199.99	200.53	201.79	202.37	204.67
23		210.01	210.98	211.84	212.81	215.14	216.21
24		222.10	222.32	223.74	223.86	224.35	227.37
25		232.89	233.51	233.90	235.16	236.08	238.11

In Table 13, it is obvious that the RKGA is much more computationally efficient than the discrete MSO. The RKGA can quickly converge to the optimal solution in a small number of iterations as it is inherently combinatorial.

Fig. 7 shows the best layout of GM when $n = 13$ and $n = 25$. Compared with previous experiment results, the RKGA can provide better layouts clearly indicating the predominant wind direction. When $n = 13$, the layout presents an explicit shape of three lines. When $n = 12$, most wind turbines are located in two lines. It is clear to show the advantage of RKGA in solving GM from the quality of model solutions.

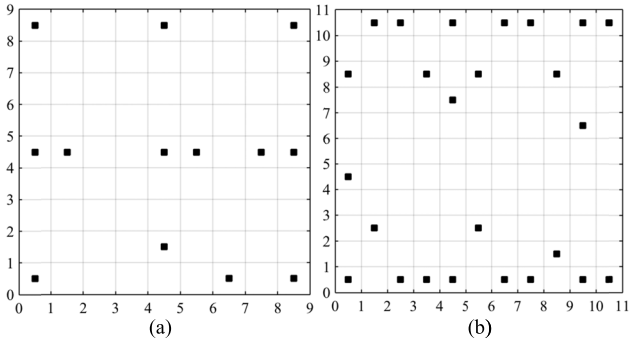

FIGURE 7. Best layout of GM with $n = 13$ and 25 in WS1 under RKGA. (a) $n = 13$. (b) $n = 25$.

VII. CONCLUSION

This research assessed the effectiveness of GM and CM for the wind farm layout design. The formulations of grid and coordinate wind farm layout models were presented. The computational complexity of solving GM and CM with the exhaustive search was theoretically analyzed. Computational studies were conducted to examine the impact of more advanced heuristic search algorithms on solving two models. To compare the performances of GM and CM, the MSO algorithm was applied. To evaluate the importance of selecting correct algorithms, the RKGA was compared with MSO algorithm in solving GM. Case studies based on different wind scenarios were investigated and the results were reported.

Through the theoretical analyses, we proved that solving CM is more complicated than GM with the exhaustive search. Based on computational results of different cases in wind scenarios 1 and 2, the following insights were discovered: 1) the performance of CM was better than GM on maximizing the power output and computational time in most cases under MSO. Besides the flexibility of CM, the MSO, which is inherently continuous, is more suitable for solving the continuous problem than the combinational problem; 2) when the number of wind turbines was low, the optimal solutions were not unique and easy to be searched for both of GM and CM; 3) an extremely large number of grid cells might affect the quality of the generated wind farm layout based on GM because the pool of feasible solutions expanded and the effectiveness of heuristic algorithms degraded; 4) it was important to match the inherent suitability of heuristic search algorithms with the type of the layout planning models.

REFERENCES

[1] L. Vermeer, J. N. Sørensen, and A. Crespo, "Wind turbine wake aerodynamics," *Prog. Aerosp. Sci.*, vol. 39, nos. 6–7, pp. 467–510, 2003.
[2] G. Mosetti, C. Poloni, and B. Diviacco, "Optimization of wind turbine positioning in large windfarms by means of a genetic algorithm," *J. Wind Eng. Ind. Aerodyn.*, vol. 51, no. 1, pp. 105–116, 1994.
[3] S. A. Grady, M. Y. Hussaini, and M. M. Abdullah, "Placement of wind turbines using genetic algorithms," *Renew. Energy*, vol. 30, no. 2, pp. 259–270, 2005.
[4] J. Calero-Barón, J. Riquelme-Santos, and M. Burgos-Payán, "An evolutive algorithm for wind farm optimal design," *Neurocomputing*, vol. 70, nos. 16–18, pp. 2651–2658, 2007.
[5] B. L. Du Pont and J. Cagan, "An extended pattern search approach to wind farm layout optimization," *J. Mech. Design*, vol. 134, no. 8, p. 081002, 2012.
[6] A. Emami and P. Noghreh, "New approach on optimization in placement of wind turbines within wind farm by genetic algorithms," *Renew. Energy*, vol. 35, no. 7, pp. 1559–1564, 2010.
[7] H. Long and Z. Zhang, "A two-echelon wind farm layout planning model," *IEEE Trans. Sustain. Energy*, vol. 6, no. 3, pp. 863–871, Jul. 2015.
[8] Y. Chen, H. Li, B. He, P. Wang, and K. Jin, "Multi-objective genetic algorithm based innovative wind farm layout optimization method," *Energy Convers. Manage.*, vol. 105, pp. 1318–1327, 2015.
[9] A. Kusiak and Z. Song, "Design of wind farm layout for maximum wind energy capture," *Renew. Energy*, vol. 35, no. 3, pp. 685–694, 2010.
[10] B. Saavedra-Moreno, S. Salcedo-Sanz, A. Paniagua-Tineo, L. Prieto, and A. Portilla-Figueras, "Seeding evolutionary algorithms with heuristics for optimal wind turbines positioning in wind farms," *Renew. Energy*, vol. 36, no. 11, pp. 2838–2844, 2011.
[11] Y. Eroğlu and S. U. Seçkiner, "Design of wind farm layout using ant colony algorithm," *Renew. Energy*, vol. 44, pp. 53–62, Aug. 2012.
[12] B. Pérez, R. Mínguez, and R. Guanche, "Offshore wind farm layout optimization using mathematical programming techniques," *Renew. Energy*, vol. 53, pp. 389–399, May 2013.
[13] S. Chowdhury, J. Zhang, A. Messac, and L. Castillo, "Optimizing the arrangement and the selection of turbines for wind farms subject to varying wind conditions," *Renew. Energy*, vol. 52, pp. 273–282, Apr. 2013.
[14] S. Salcedo-Sanz, B. Saavedra-Moreno, A. Paniagua-Tineo, L. Prieto, and A. Portilla-Figueras, "A review of recent evolutionary computation-based techniques in wind turbines layout optimization problems," *Central Eur. J. Comput. Sci.*, vol. 1, no. 1, pp. 101–107, 2011.
[15] Y. Eroğlu, "Wind farm layout design optimization: Continuous versus discrete search spaces," in *Proc. 19th Future Res. Combinat. Optim. (FRICO)*, 2015, p. 13.
[16] N. O. Jensen, "A note on wind generator interaction," Dept. Wind Energy, Risø Nat. Lab., Tech. Univ. Denmark, Roskilde, Denmark, Tech. Rep. M-2411, 1983.
[17] S. Z. Zhao, J. Liang, P. Suganthan, and M. F. Tasgetiren, "Dynamic multi-swarm particle swarm optimizer with local search for large scale global optimization," in *Proc. IEEE World Congr. Comput. Intell. Evol. Comput.*, Jun. 2008, pp. 3845–3852.
[18] J. Kennedy, "Particle swarm optimization," in *Encyclopedia of Machine Learning Anonymous*. New York, NY, USA: Springer, 2010, pp. 760–766.
[19] J. Kennedy and R. C. Eberhart, "A discrete binary version of the particle swarm algorithm," in *Proc. IEEE Int. Conf. Syst., Man*, Oct. 1997, pp. 4104–4108.
[20] J. C. Bean, "Genetic algorithms and random keys for sequencing and optimization," *ORSA J. Comput.*, vol. 6, pp. 154–160, May 1994.

HUAN LONG (S'16) received the B.S. degree from the Department of Automation, Huazhong University of Science and Technology, China, in 2013. She is currently pursuing the Ph.D. degree with the Systems Engineering and Engineering Management Department, City University of Hong Kong, Hong Kong, China. Her research includes data mining and computational intelligence applied in the renewable energy optimization, such as wind farm layout, hybrid renewable system configuration, renewable energy prediction, and wind turbine monitoring.

ZIJUN ZHANG (M'12) received the B.Eng. degree in systems engineering and engineering management from The Chinese University of Hong Kong, Hong Kong, China, in 2008, and the M.S. and Ph.D. degrees in industrial engineering from The University of Iowa, USA, in 2009 and 2012, respectively.

He is currently an Assistant Professor with the Department of Systems Engineering and Engineering Management, City University of Hong Kong, Hong Kong. His research focuses on data mining and computational intelligence with applications in the modeling, monitoring, optimization, and operations of systems in wind energy, HVAC, and wastewater processing domains. He is an Associate Editor of the *Journal of Intelligent Manufacturing*.

ZHE SONG received the Ph.D. degree in industrial engineering from The University of Iowa in 2008. He was a Post-Doctoral Researcher with The University of Iowa. He joined the School of Business, Nanjing University, as an Associate Professor in 2009. His research interests include operations research, data mining, control theory, computational intelligence, and their applications in business, energy and manufacturing systems modeling and optimization, such as mass customization, power plant performance optimization, wind power management, optimal decision making in heating ventilating and air conditioning.

ANDREW KUSIAK (M'88) received the B.S. and M.S. degrees in precision engineering from the Warsaw University of Technology, Warsaw, Poland, in 1972 and 1974, respectively, and the Ph.D. degree in operations research from the Polish Academy of Sciences, Warsaw, in 1979.

He is currently a Professor with the Intelligent Systems Laboratory, Department of Mechanical and Industrial Engineering, The University of Iowa, USA. He has authored or co-authored numerous books and technical papers in journals sponsored by professional societies, such as the Association for the Advancement of Artificial Intelligence, the American Society of Mechanical Engineers, Institute of Industrial and Systems Engineers, and other societies. His current research interests include the application of computational intelligence in automation, renewable energy, smart manufacturing, product development, and healthcare. He is a fellow of the Institute of Industrial and Systems Engineers and the Editor-in-Chief of the *Journal of Intelligent Manufacturing*. He has served on the Editorial Board of over 50 journals.